J Nanopart Res (2015) 17:114
DOI 10.1007/s11051-015-2916-6

RESEARCH PAPER

# Photocatalytic oxidation of propylene on La and N codoped $TiO_2$ nanoparticles

**Jinfeng Liu · Haiyan Li · Lanlan Zong · Qiuye Li · Xiaodong Wang · Min Zhang · Jianjun Yang**

Received: 21 December 2014 / Accepted: 12 February 2015 / Published online: 28 February 2015


**Abstract** Lanthanum- and nitrogen-codoped $TiO_2$ photocatalysts was synthesized using orthorhombic nanotubes titanic acid as the precursor by a simple impregnation and subsequent calcination method. The morphology, phase structure, and properties of La- and N-codoped $TiO_2$ were well characterized by transmission electron microscopy, X-ray diffraction, Raman spectra, X-ray photoelectron spectroscopy, and UV–Vis diffuse reflectance spectra. The La-/N-codoped $TiO_2$ showed excellent photoactivity of propylene oxidation compared with the single-doped $TiO_2$ and La-/N-codoped P25 $TiO_2$ nanoparticles under visible light irradiation. The origin of the enhancement of the visible light-responsive photocatalytic activity was discussed in detail.

**Keywords** Nanotube titanic acid · La, N-codoped $TiO_2$ · Propylene oxidation · Visible light · Nanostructured catalysts

J. Liu · H. Li · L. Zong · Q. Li (✉) · X. Wang · M. Zhang · J. Yang (✉)
Key Laboratory for Special Functional Materials, Henan University, Kaifeng 475004, China
e-mail: lqybys@163.com

J. Yang
e-mail: yangjianjun@henu.edu.cn

## Introduction

Recently, the increasingly serious environmental problems have been attracted much attention by several researchers. Some new nanomaterials have been prepared to govern environmental pollution by photocatalytic method (Du et al. 2013; Wang et al. 2013). Photocatalysis of $TiO_2$ for environmental remediation has been widely concerned for several decade years due to its advantages of being inexpensive, nontoxic, and good chemical stability. However, two shortages have limited its practical application. One is the large band gap energy (Eg = 3.2 eV), and the other is the low quantum efficiency of the photogenerated charge carries. In order to improve the visible light-responsive photocatalytic activity, doping $TiO_2$ with metal or nonmetal elements is a popular method (Asahi et al. 2001; Dana Dvoranová et al. 2002; Huang et al. 2007; Park et al. 2006; Umebayashi et al. 2003). Among the nonmetal-doped researches, doping with nitrogen is considered as an effective method to increase the absorption and improve the activity. Wang et al. prepared N-doped $TiO_2$ by annealing different Ti precursors in flowing $NH_3$, indicated that doping with nitrogen could enhance the absorption of visible light effectively (Wang et al. 2011). For the metal-doped $TiO_2$, especially, rare-earth metal-doped $TiO_2$ has attracted much attention in visible light-responded photocatalysis. Lanthanide ions showed special optical properties and extraordinary catalytic capacity owing to its special electronic

structure of 4fx 5dy. Incorporation of lanthanide ions in $TiO_2$ matrix could provide a means to adsorb the organic pollutants on the semiconductor surface and therefore enhanced the photocatalytic activity (Xu et al. 2009). Hou et al. synthesized a highly active La-doped $TiO_2$ photocatalyst for the degradation of phenol by ultrasound-assisted sol–gel method. The incorporation of La might facilitate the adsorption for reactant molecules and UV lights, and also inhibit the recombination between photoelectrons and holes, leading to the higher photocatalytic activity (Huo et al. 2007). Single doping with metal or nonmetal has made some progress, but the photocatalytic efficiency still very low. Nitrogen doping can expand photo-absorption effectively, and the metal doping can improve the separation of the photo-generated electron–hole pairs. If $TiO_2$ can be doped by nitrogen and metal, the photocatalytic activity may have a large improvement. Cong and coworkers prepared nitrogen- and lanthanum-codoped titania nanocrystals, and found that nitrogen doping could narrow the band gap of titania and enhance the utilization efficiency of visible light, while the $La^{3+}$ dopant could accelerate the separation of photo-generated electrons and holes. The codoped photocatalysts showed higher photocatalytic activities than pure $TiO_2$ and single-component nitrogen- or lanthanum-doped $TiO_2$ (Cong et al. 2011). However, the previously reported codoped $TiO_2$ was often obtained by the sol–gel and calcination method, and their small BET surface areas can only provide very less-active sites for the pollutants, and thereby the photocatalytic activity was relatively lower.

Recently, nanotubes titanic acid (NTA) attracted much attention due to many excellent properties, such as large BET surface area, strong absorption capability, ion-exchange capacity, one-dimensional structure, and so on. The formation mechanism, photoelectrochemical properties, and thermal dehydrated characters were systematically investigated in our former work (Li et al. 2007, 2006; Wang et al. 2010; Xing et al. 2012; Yang et al. 2003; Zhang et al. 2011, 2004). NTA can transform to a novel anatase $TiO_2$ by dehydration, and this kind of $TiO_2$ possess a large amount of single-electron-trapped oxygen vacancies (SETOV), and which can be excited by the visible light. And they also have larger BET surface area than the well-known P25. It is most important that SETOV can make the nitrogen dopant more stable and increase the doping amount (Irie et al. 2003).

In this work, La- and N-codoped $TiO_2$ were prepared using NTA and P25 as titanium precursor. This kind of La, N-doped $TiO_2$ showed much higher activity than the single-doped $TiO_2$ and codoped P25. A systemic investigation was employed to reveal the effects of La and N dopants in the enhancement of the visible light absorption and photoactivity for propylene oxidation.

## Experimental

### Preparation of samples

The titania precursor of NTA was prepared according to our previous reports (Feng et al. 2012; Zhang et al. 2004). A certain quantity of NTA and urea (mass ratio of 2:1) were added into 60 mL of de-ionized water, then the pre-calculated amount of $La(NO_3)_3$ was added under stirring for 4 h (the atomic ratio of La/Ti equals to 0, 0.1, 0.3, 0.5, 1.0, and 3.0 %, respectively). The resultant mixed solution transferred to the round-bottom flask to evaporate water by a vacuum distillation. The obtained product was calcinated at 500 °C for 4 h, and they were donated as x %La/N-$TiO_2$. The single-doped La-$TiO_2$ and N-$TiO_2$ were synthesized using the similar process but without the addition of urea or lanthanum nitrate, respectively. For comparison, Degussa P25 powders were also selected to prepare La, N-codoped $TiO_2$ under the same conditions (denoted as La/N-P25).

### Characterization

The phase composition of various x %La/N-$TiO_2$ samples were analyzed by X-ray diffraction (XRD, Philips X'Pert Pro X-ray diffractometer; Cu Kα radiation, $\lambda = 0.15$ nm). The X-ray photoelectron spectroscopic (XPS) measurement was carried out using ESCALAB210 with dual-anode Mg X-ray source. All spectra were calibrated to the binding energy of the adventitious C 1 s peak at 285 eV. The UV–Vis diffuse reflectance spectra were obtained on a Shimadzu U-3010 spectrometer, using $BaSO_4$ as a reference. The morphology of the samples was taken on a transmission electron microscopy (TEM, JEOL JEM-2100, accelerating voltage 200 kV). The Brunauer–Emmett–Teller (BET) surface areas and average pore volumes were measured by automatic surface

area and porosity analyzer (QUADRASORB SI). The photoluminescence (PL) spectra were recorded on a fluorescence spectrometer.

### Photocatalytic activity measurements

The photocatalytic activity was evaluated by measuring the oxidation of propylene (the initial concentration was ca. 600 ppm, and the flow rate was ca. 150 mL/h) under visible light irradiation. A 300 W xenon lamp with a cutoff filter ($\lambda \geq 420$ nm) was used as the visible light source. About 25 mg of photocatalyst was spread on one side of a glass plate (ca. 8.4 $cm^2$ active areas) and kept in a flat quartz tube reactor. The concentration of $C_3H_6$ was determined at a sensitivity of 1 ppm (v/v over volume) using a chromatograph (ShimadzuGC-9A) equipped with a flame ionization detector, a GDX-502 column, and a reactor loaded with Ni catalyst for the methanization of $CO_2$. Prior to irradiation, an adsorption and desorption equilibrium of $C_3H_6$ was established. The photocatalytic activity of visible light photocatalytic oxidation of $C_3H_6$ was calculated as $(C_0-C)/C_0 \times 100$ %, where $C_0$ refers to the concentration of $C_3H_6$.

## Results and discussions

The XRD patterns of the series of La/N doped $TiO_2$ are shown in Fig. 1. The typical diffraction peaks at 25.3°, 37.8°, 48.0°, 53.9°, 55.0°, and 62.7° are corresponded to the (101), (104), (200), (105), (211), and (204) plane facet of anatase $TiO_2$, respectively. Our previous work has reported that NTA belongs to a orthorhombic crystallinity (Yang et al. 2003). From the above XRD results, we knew that NTA has transformed to $TiO_2$ completely through the simple calcination process. The character peaks of x %La/N-$TiO_2$ have no obvious difference with the pure anatase $TiO_2$. Raman spectroscopy is more sensitive to the surface region of $TiO_2$. Figure 2 shows the Raman spectra of the pure $TiO_2$ and 3 %La/N-$TiO_2$ samples. The bands at 141 $cm^{-1}$ (Eg), 393 $cm^{-1}$ (B1 g), 519 $cm^{-1}$ (B1 g), and 636 $cm^{-1}$ (Eg) are attributed to anatase phase (Boppella et al. 2012). This result is consistent with XRD analysis. Slight shift of peak position at 141 $cm^{-1}$ is observed in the inset picture. This is due to the existence of small amounts of lanthanum doped into crystal lattice of the titanium dioxide.

The structural and morphological study was completed with the help of TEM technique. As shown in Fig. 3a, NTA displays uniform nanotube structure, the diameters of NTA are about 6–10 nm, and the length can reach several micrometers. After calcination, as shown in Fig. 3b, the shape of the tube was destroyed and converted into small particles completely.

The optical absorption property of the sample was measured through the UV–Vis diffuse reflection spectra, as shown in Fig. 4. There is no visible light absorption for P25 and the undoped $TiO_2$. Absorption band edge of all other samples prepared by NTA exhibits clear shifts to the visible region after calcination, especially for N-doped $TiO_2$. Our previous

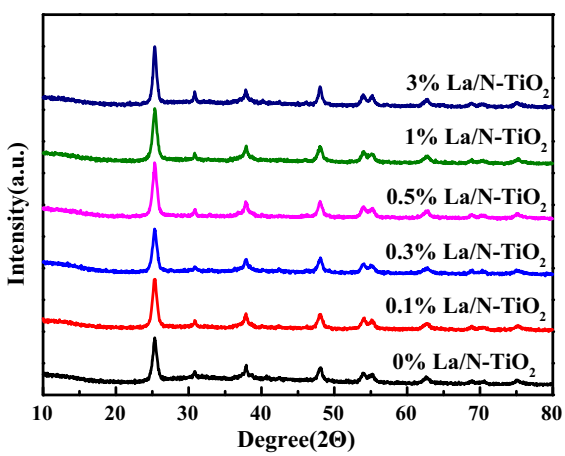


**Fig. 1** XRD patterns of the x %La/N-$TiO_2$ samples

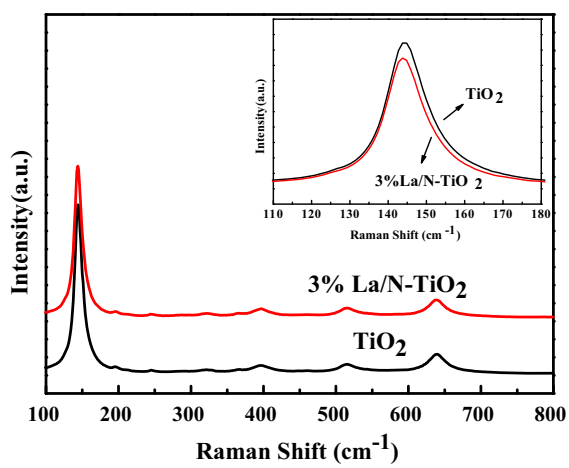


**Fig. 2** Raman spectra of undoped $TiO_2$ and 3 %La/N-$TiO_2$

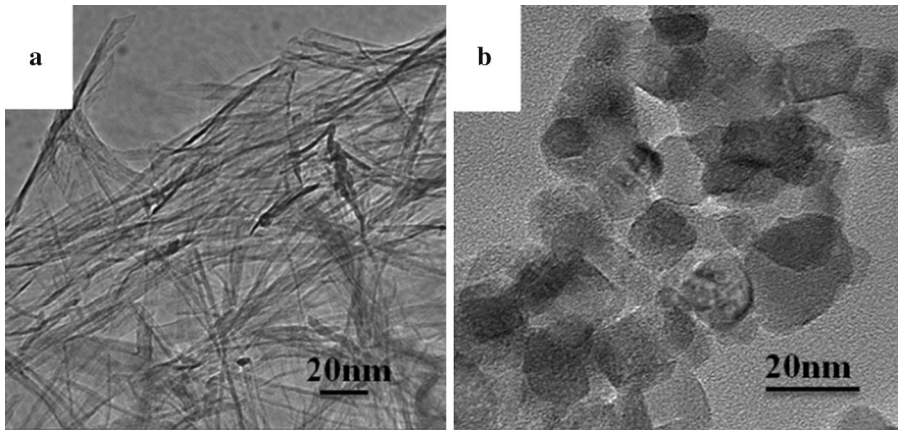


**Fig. 3** TEM images of **a** NTA precursor and **b** 0.3 %La/N-$TiO_2$

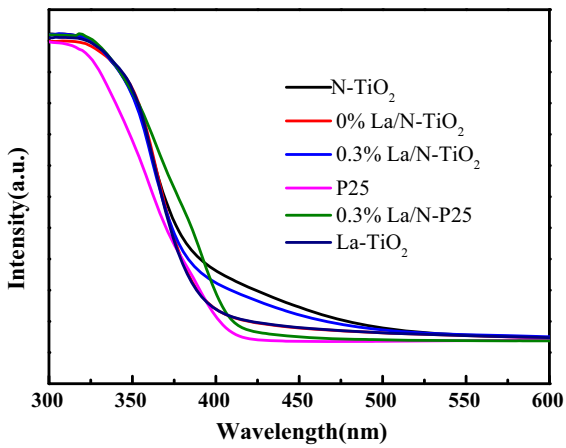


**Fig. 4** UV–Vis diffuse reflectance spectra of samples

work has verified that a large amount of SETOV could be generated in the high-temperature dehydration process, which could broaden the absorption light to the visible light region. The optical absorption of the pure $TiO_2$ and La-doped $TiO_2$ using NTA as the precursor has no obvious difference. However, the absorption band edge of 0.3 %La/N-$TiO_2$ expanded to the visible light region compared to the undoped $TiO_2$. Interestingly, the visible light absorption of 0.3 %La/N-$TiO_2$ was much higher than that of the 0.3 %La/N-P25. This implied that NTA is a better precursor to prepare high visible light-responsive doped $TiO_2$ than P25 (Zhang et al. 2013).

XPS analysis is conducted to understand the surface chemical state of La-/N-doped $TiO_2$ nanoparticles. The spectrum of La 3d of 0.3 %La/N-$TiO_2$ is shown in Fig. 5a. The two peaks centered at 834.2 and 853.5 eV are attributed to La 3d5/2 and La 3d3/2, respectively (Zong et al. 2013), which proved the existence of lanthanum. Two characteristic peaks of Ti 2p of undoped $TiO_2$ appeared at 458.4 and 464.1 eV just as shown in Fig. 5b, which indexed to Ti 2p1/2 and Ti 2p3/2, respectively. This indicates that the Ti exists in the form of $Ti^{4+}$ (Gao et al. 2010). The binding energy of $Ti^{3+}$ is lower than those of $Ti^{4+}$ about 1.8 eV (Price et al. 1999), which is not observed in the Ti 2p XPS spectra. The binding energy of Ti 2p of N-$TiO_2$ and 0.3 %La/N-$TiO_2$ shifts to higher value compared with undoped $TiO_2$. This change suggests the different electronic interactions of Ti ions (Huang et al. 2009), which justifies the incorporation of La and N into the crystal lattice of titanium dioxide (Lan et al. 2014). The dopant $La^{3+}$ could effectively inhibit the recombination of carriers. The spectrum of N 1 s is presented in Fig. 5c. To date, the assignment of the XPS peak of N 1 s has still been under debate. In many cases, the peak locates at about 399.7 and 396 eV are attributed to substitutional and interstitial nitrogen species, respectively (Shen et al. 2008). Previous studies in our group have found that the concentration of oxygen vacancy could increase with increase of nitrogen content. Thus, doping with nitrogen could improve the photocatalytic activity in the visible light region. The peak at about 402.9 eV indicated that a small amount of N species was in the form of C–N bond (Kubacka et al. 2009).

Figure 6 shows the $N_2$ adsorption–desorption isotherms of undoped $TiO_2$ and 0.3 %La/N-$TiO_2$.

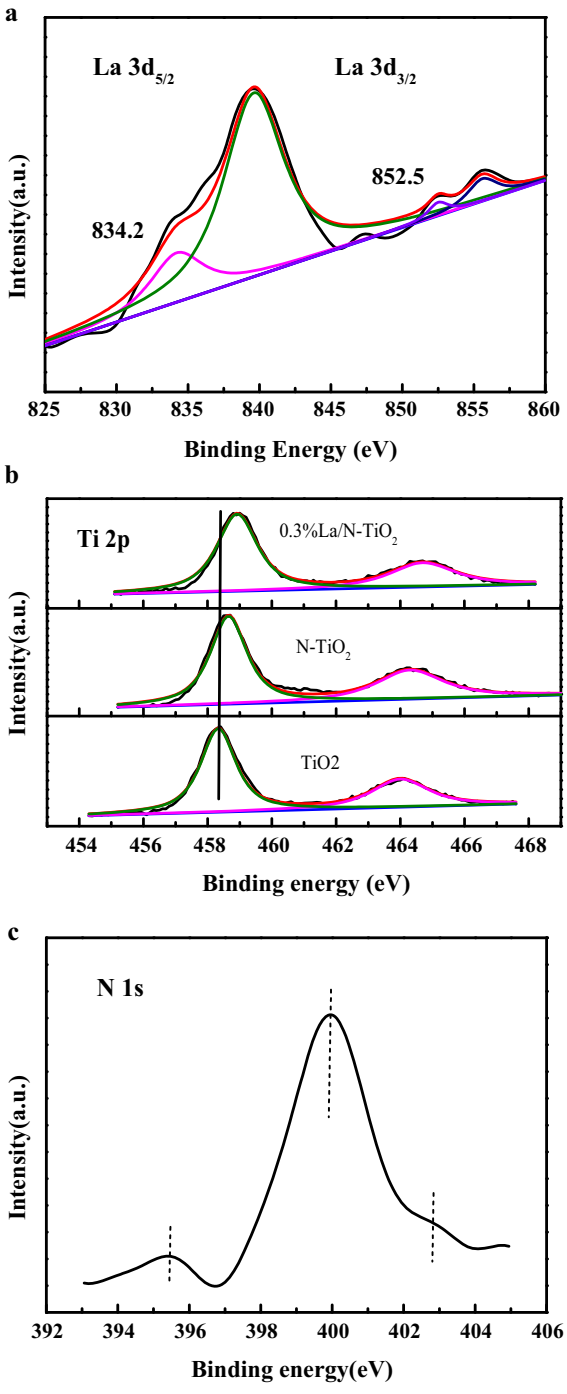


**Fig. 5** XPS spectra of **a** La 3d in 0.3 %La/N-$TiO_2$, **b** N 1 s in 0.3 %La/N-$TiO_2$, **c** Ti 2p in undoped $TiO_2$, N-$TiO_2$, and 0.3 %La/N-$TiO_2$

The samples show a typical type-IV isotherm with an H3 type hysteresis loop (Wang et al. 2009), indicating the existence of mesoporous structure of samples. The

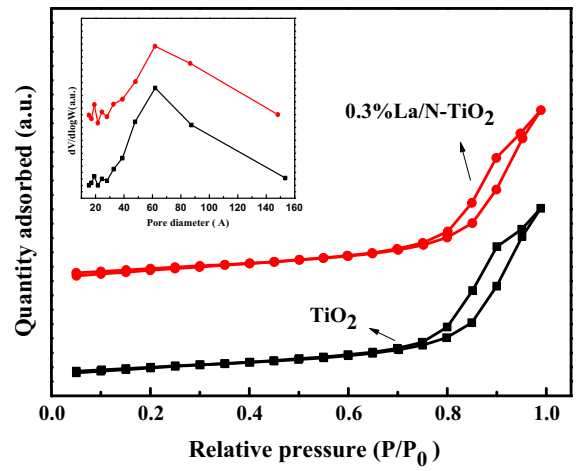


**Fig. 6** Nitrogen adsorption–desorption isotherms of undoped $TiO_2$ and 0.3 %La/N-$TiO_2$, and the *inset* figure displays pore size distribution of undoped $TiO_2$ and 0.3 %La/N-$TiO_2$

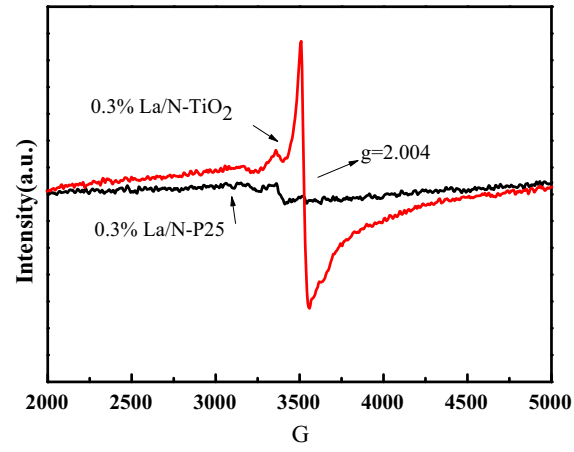


**Fig. 7** ESR spectra of 0.3 %La/N-$TiO_2$ and 0.3 %La/N-P25

pore size distribution acquired using the BJH method is given in inset picture. The pore size distributions of $TiO_2$ and 0.3 %La/N-$TiO_2$ are mainly in the range of 4–12 nm. The BET surface area of 0.3 %La/N-$TiO_2$ is much larger than that of 0.3 %La/N-P25, corresponding to 101 and 54 $m^2g^{-1}$, respectively. The large surface area could provide much more adsorption sites for pollutants, which in favor of the improvement of the photocatalytic activity.

Electron spin resonance (ESR) spectra of 0.3 %La/N-$TiO_2$ and 0.3 %La/N-P25 are shown in Fig. 7. No characteristic ESR signal of $Ti^{3+}$ ($g = 1.96$) ion was

detected, well corresponding to the absence of $Ti^{3+}$ species in relevant XPS analysis. In 0.3 %La/N-$TiO_2$ samples, there is a strong characteristic ESR signal ($g = 2.004$) that can be seen, which demonstrated the presence of SETOV (Sakatani et al. 2003; Wang et al. 2011). SETOV are mainly generated from dehydration process of NTA, which is beneficial for the adsorption of visible light. However, characteristic ESR signal of SETOV could not be found in 0.3 %La/N-P25. This indicates that 0.3 %La/N-$TiO_2$ may have a higher visible light photocatalytic performance than 0.3 %La/N-P25, and it is proved by the activity results discussed below.

Photodegradation of $C_3H_6$ was used as the probe reaction to evaluate the photocatalytic activity of samples under visible light irradiation (Fig. 8a). The degradation yield of $C_3H_6$ on undoped $TiO_2$ was 13 %. All the La/N-$TiO_2$ samples showed relatively higher visible light photocatalytic performance compared with undoped $TiO_2$. With the increase of lanthanum content, the photocatalytic activities of La/N-$TiO_2$ samples increased. Then the degradation yield decreased to about 16 % with the increased lanthanum doping amount up to 3 %. The optimal doping of lanthanum ion at 0.3 % corresponding to the degradation yield of propylene is 35 %, which might be due to the fact that there was an optimal doping of lanthanum ions in titania particles for the most efficient separation of photo-generated electron and hole pairs.

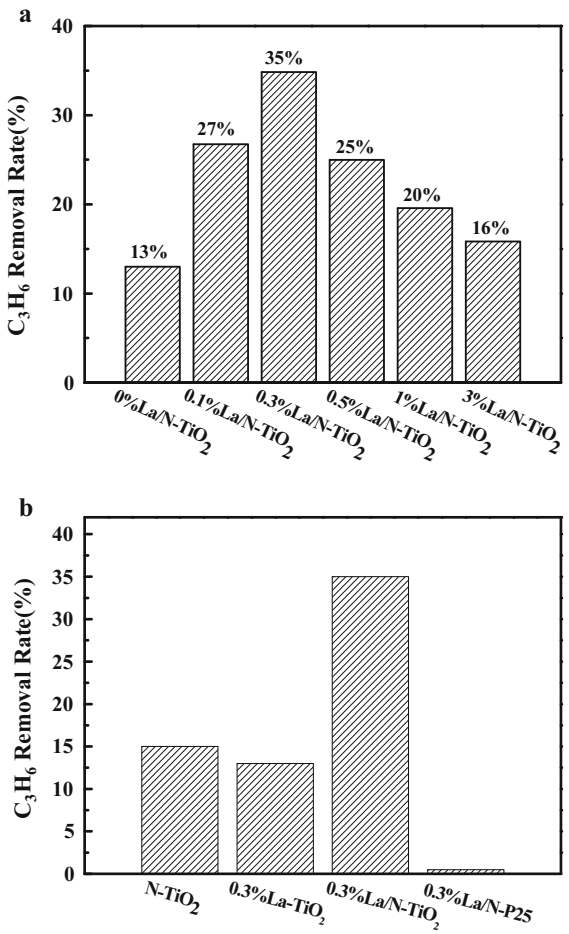


**Fig. 8** Visible light photocatalytic activity of **a** x %La/N-$TiO_2$; **b** N-$TiO_2$, La-$TiO_2$, 0.3 %La/N-$TiO_2$, 0.3 %La/N-P25

For comparison, Degussa P25 was also used as a precursor to prepare doped $TiO_2$ samples. Figure 8b shows the degradation yield of $C_3H_6$ on 0.3 %La-$TiO_2$, N-$TiO_2$, 0.3 %La/N-$TiO_2$, and 0.3 %La/N-P25. The sample of 0.3 %La/N-$TiO_2$ exhibits excellent performance compared with single-component doping $TiO_2$ and 0.3 %La/N-P25. An energy level (N 2p) is introduced just above the valence band so as to absorb more visible light. And the $La^{3+}$ dopant can improve the separation efficiency of the photo-generated electron–hole pairs. Combining the role of N and $La^{3+}$, the 0.3 %La/N-$TiO_2$ showed an excellent visible light activity. The degradation yield of $C_3H_6$ on 0.3 %La/N-$TiO_2$ is 35 %, whereas 0.3 % La/N-P25 almost no visible light activity. The main reasons for this difference are given as follows. Firstly, in our previous work, we reported that the anatase $TiO_2$ obtained from the dehydration of NTA possessed a large amount of SETOV. This kind of $TiO_2$ with SETOV could increase the capacity of absorption of visible light and improve the visible light photocatalytic activity. Secondly, the excited electrons could be capped by the defects generated by the dopant atoms which improved the separation efficiency of the electrons and holes. Thirdly, the larger surface area could adsorb more contaminants and provide more active sites, which is beneficial for the improvement of the catalytic activity of the visible light.

Based on the above experimental results, a possible mechanism for the degradation of $C_3H_6$ is proposed in Scheme 1. This kind of $TiO_2$ obtained by dehydration of NTA can be excited by the visible light because of the existence of the sub-band (SETOV) (Zong et al. 2013). An energy level (N 2p) was introduced just above the valence band so as to absorb more visible

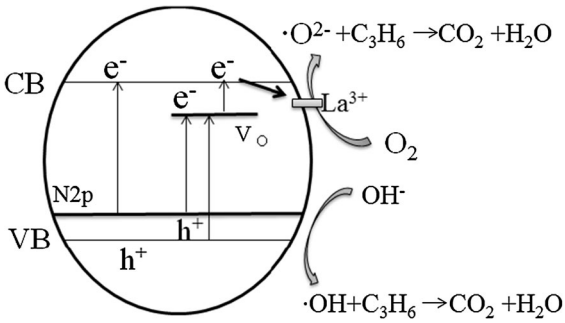


**Scheme1** Mechanism for the degradation of $C_3H_6$

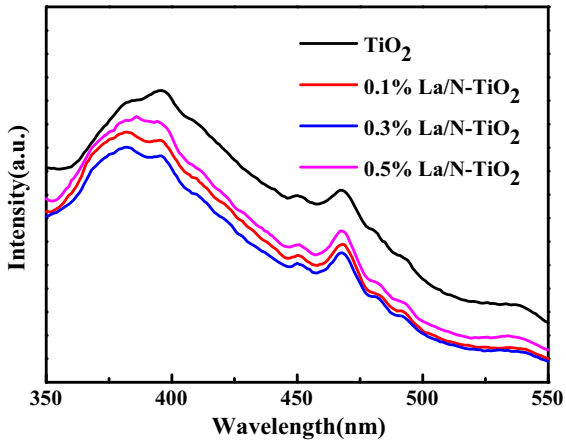


**Fig. 9** PL spectra of the undoped $TiO_2$, 0.1 % La/N-$TiO_2$, 0.3 %La/N-$TiO_2$, 0.5 % La/N-$TiO_2$

light. Under visible light irradiation, the electrons could be excited into conduction band of $TiO_2$ by several steps. The $La^{3+}$ dopant can improve the separation efficiency of the photo-generated electron–hole pairs. Subsequently, the electrons were scavenged by surface-absorbed $O_2$ to form superoxide radical ($O_2^-$). The produced holes shifted to the surface and combine with OH- absorbed on the surface of La/N-$TiO_2$ and resulted in the formation of OH·. Decomposition of $C_3H_6$ was accomplished by those oxide species.

Photoluminescence (PL) emission spectrum is a method used to study the transfer behavior of the photo-generated electrons and holes and understand the separation and recombination of photo-generated charge carriers (Zhang et al. 2000). As shown in Fig. 9, the PL intensity of $TiO_2$ decreased greatly after codoped lanthanum and nitrogen, while the undoped $TiO_2$ has a highest PL intensity. This indicated that the recombination rate of the photo-generated electrons and holes on La, N-doped $TiO_2$ is lower than pure $TiO_2$. Moreover, the 0.3 %La/N-$TiO_2$ is the lowest, which would lead to a higher photocatalytic activity. Therefore, the PL result was consistent with the actual photocatalytic activity.

## Conclusions

Lanthanum- and nitrogen-codoped $TiO_2$ was synthesized using orthorhombic NTA as the precursor by a simple impregnation and subsequent calcination method. x %La/N-$TiO_2$ showed excellent photocatalytic activity compared with single-doped NTA and La/N-P25 for the oxidation of propylene under visible light irradiation. The XRD and Raman results indicated that NTA was transported to anatase completely, and lanthanum doped into crystal lattice of the titanium dioxide. $N_2$ adsorption–desorption analysis revealed that the samples belonged to mesoporous structure and had large surface area than doped P25. The EPR results indicated that large amount of SETOV possessed in La-/N-codoped $TiO_2$, while it was absent in La-/N-codoped P25. $TiO_2$ with SETOV could increase the capacity of absorption of visible light and improve the visible light photocatalytic activity. What is more is that the large surface areas could provide much more adsorption sites for pollutant molecules, which in favor of the improvement of the photocatalytic activity.

**Acknowledgments** The authors gratefully acknowledge the support of the National Natural Science Foundation of China (Nos. 21103042, 21471047, 21203054), Program for Science & Technology Innovation Talents in Universities of Henan Province (No. 15HASTIT043), and Program for Changjiang Scholars and Innovation Research Team in University (No. PCS IRT1126).

## References

Asahi R, Morikawa T, Ohwaki T, Aoki K, Taga Y (2001) Visible-light photocatalysis in nitrogen-doped titanium oxides. Science 293:269–271

Boppella R, Basak P, Manorama SV (2012) Viable method for the synthesis of biphasic TiO2 nanocrystals with tunable phase composition and enabled visible-light photocatalytic performance. ACS Appl Mater Interfaces 4:1239–1246. doi:10.1021/am201354r

Cong Y, Tian B, Zhang J (2011) Improving the thermal stability and photocatalytic activity of nanosized titanium dioxide via $La^{3+}$and N co-doping. Appl Catal B 101:376–381. doi:10.1016/j.apcatb.2010.10.006

Dana Dvoranová VB, Mazúra Milan, Malati Mounir A (2002) Investigations of metal-doped titanium dioxide photocatalysts. Appl Catal B 37:91–105. doi:10.1016/S0926-3373(01)00335-6

Du W et al (2013) ZrO2/Dy2O3 solid solution nano-materials: tunable composition, visible light-responsive photocatalytic activities and reaction mechanism. J Am Ceram Soc 96:2979–2986. doi:10.1111/jace.12414

Feng C, Wang Y, Zhang J, Yu L, Li D, Yang J, Zhang Z (2012) The effect of infrared light on visible light photocatalytic activity: an intensive contrast between Pt-doped TiO2 and N-doped TiO2. Appl Catal B 113–114:61–71. doi:10.1016/j.apcatb.2011.09.027

Gao X, Jiang Y, Zhong Y, Luo Z, Cen K (2010) The activity and characterization of CeO2-TiO2 catalysts prepared by the sol-gel method for selective catalytic reduction of NO with NH3. J Hazard Mater 174:734–739. doi:10.1016/j.jhazmat.2009.09.112

Huang D, Liao S, Quan S, Liu L, He Z, Wan J, Zhou W (2007) Preparation of anatase F doped TiO2 sol and its performance for photodegradation of formaldehyde. J Mater Sci 42:8193–8202

Huang Y, Ho W, Ai Z, Song X, Zhang L, Lee S (2009) Aerosol-assisted flow synthesis of B-doped, Ni-doped and B-Ni-codoped TiO2 solid and hollow microspheres for photocatalytic removal of NO. Appl Catal B 89:398–405

Huo Y, Zhu J, Li J, Li G, Li H (2007) An active La/TiO2 photocatalyst prepared by ultrasonication-assisted sol–gel method followed by treatment under supercritical conditions. J Mol Catal A 278:237–243. doi:10.1016/j.molcata.2007.07.054

Irie H, Watanabe Y, Hashimoto K (2003) Nitrogen-concentration dependence on photocatalytic activity of TiO2-xNx powders. J Phys Chem B 107:5483–5486. doi:10.1021/jp030133h

Kubacka A, Bn Bachiller-Baeza, Colón G, Fernández-García M (2009) W, N-codoped TiO2-anatase: a sunlight-operated catalyst for efficient and selective aromatic hydrocarbons photo-oxidation. J Phys Chem C 113:8553–8555. doi:10.1021/jp902618g

Lan X, Wang L, Zhang B, Tian B, Zhang J (2014) Preparation of lanthanum and boron co-doped TiO2 by modified sol–gel method and study their photocatalytic activity. Catal Today 224:163–170. doi:10.1016/j.cattod.2013.10.062

Li QY, Zhang JW, Jin ZS, Yang DG, Wang XD, Yang JJ, Zhang ZJ (2006) Photo and photoelectrochemical properties of p-type low-temperature dehydrated nanotube titanic acid. Electrochem Commun 8:741–746. doi:10.1016/j.elecom.2006.03.002

Li QY et al (2007) n/p-Type changeable semiconductor TiO2 prepared from NTA. J Nanopart Res 9:951–957. doi:10.1007/s11051-006-9095-4

Park JH, Kim S, Bard AJ (2006) Novel carbon-doped TiO2 nanotube arrays with high aspect ratios for efficient solar water splitting. Nano Lett 6:24–28

Price NJ, Reitz JB, Madix RJ, Solomon E (1999) A synchrotron XPS study of the vanadia–titania system as a model for monolayer oxide catalysts. J Electron Spectrosc Relat Phenom 98:257–266

Sakatani Y et al (2003) Photocatalytic decomposition of acetaldehyde under visible light irradiation over $La^{3+}$ and N co-doped TiO2. Chem Lett 32:1156–1157. doi:10.1246/cl.2003.1156

Shen Y, Xiong T, Li T, Yang K (2008) Tungsten and nitrogen co-doped TiO2 nano-powders with strong visible light response. Appl Catal B 83:177–185. doi:10.1016/j.apcatb.2008.01.037

Umebayashi T, Yamaki T, Tanaka S, Asai K (2003) Visible light-induced degradation of methylene blue on S-doped $TiO_2$. Chem Lett 32:330–331

Wang Y, Huang Y, Ho W, Zhang L, Zou Z, Lee S (2009) Biomolecule-controlled hydrothermal synthesis of C-N-S-tridoped TiO2 nanocrystalline photocatalysts for NO removal under simulated solar light irradiation. J Hazard Mater 169:77–87. doi:10.1016/j.jhazmat.2009.03.071

Wang Y, Feng C, Zhang M, Yang J, Zhang Z (2010) Enhanced visible light photocatalytic activity of N-doped TiO2 in relation to single-electron-trapped oxygen vacancy and doped-nitrogen. Appl Catal B 100:84–90. doi:10.1016/j.apcatb.2010.07.015

Wang Y, Feng C, Zhang M, Yang J, Zhang Z (2011) Visible light active N-doped TiO2 prepared from different precursors: origin of the visible light absorption and photoactivity. Appl Catal B 104:268–274. doi:10.1016/j.apcatb.2011.03.020

Wang X et al (2013) Ferric phosphate hydroxide microcrystals for highly efficient visible-light-driven photocatalysts. ChemPhysChem 14:2518–2524

Xing Y, Li R, Li Q, Yang J (2012) A new method of preparation of AgBr/TiO2 composites and investigation of their photocatalytic activity. J Nanopart Res 14:1–8. doi:10.1007/s11051-012-1284-8

Xu J, Ao Y, Fu D, Yuan C (2009) Synthesis of Gd-doped TiO2 nanoparticles under mild condition and their photocatalytic activity. Colloids Surf A 334:107–111

Yang J et al (2003) Study on composition, structure and formation process of nanotube Na2Ti2O4(OH)2. Dalton Trans 20:3898–3901. doi:10.1039/b305585j

Zhang W, Zhang M, Yin Z, Chen Q (2000) Photoluminescence in anatase titanium dioxide nanocrystals. Appl Phys B 70:261–265

Zhang M et al (2004) Effect of annealing temperature on morphology, structure and photocatalytic behavior of nanotubed H2 Ti2 O4(OH)2. J Mol Catal A 217:203–210

Zhang J, Jin Z, Feng C, Yu L, Zhang J, Zhang Z (2011) ESR study on the visible photocatalytic mechanism of nitrogen-doped novel TiO2: synergistic effect of two kinds of oxygen vacancies. J Solid State Chem 184:3066–3073

Zhang M, Yu X, Lu D, Yang J (2013) Facile synthesis and enhanced visible light photocatalytic activity of N and Zr co-doped TiO2 nanostructures from nanotubular titanic acid precursors. Nanoscale Res Lett 8:543. doi:10.1186/1556-276X-8-543

Zong L, Li Q, Zhang J, Wang X, Yang J (2013) Preparation of Pd-loaded La-doped TiO2 nanotubes and investigation of their photocatalytic activity under visible light. J Nanopart Res 15:1–9. doi:10.1007/s11051-013-2042-2